

Making Sense of Measurement Geometries for Multi-angle Spectrophotometers

Eric Kirchner,^{1*} Werner Cramer²

¹AkzoNobel Car Refinishes, Technology Center Colorimetry, Rijkssstraatweg 31, 2171 AJ Sassenheim, The Netherlands

²Hafenweg 22, 48143 Münster, Germany

Received 23 August 2010; revised 5 November 2010; accepted 22 November 2010

Abstract: We have developed new parameters that help to interpret multi-angle reflection data. By expressing measurement geometries in terms of so-called flake-based parameters, a physical explanation is given for several well-known colorimetric characteristics of effect coatings. The new concepts are based on expressing angles with respect to the normal vector of flakes, instead of the conventional usage of the coating normal as a reference.

We discuss and give physical explanations for the usefulness and limitations of previously defined concepts such as aspecular angle, cis- versus trans-geometries, interference lines and aspecular lines.

For example, it is known that the trans-15° geometry has added value next to the cis+15° geometry when samples are analyzed that contain colored effect pigments with large color travel, such as Colorstream, Chromaflair, or chromatic Xirallic pigments. Our results demonstrate and explain why there is much less added value in the case of samples that contain less striking chromatic effect pigments, such as metallic or mica-based effect pigments, or “white” Xirallic pigments. Further, interference lines are shown to be suitable for characterizing effect pigments because they selectively sample the reflectance values of flakes as a function of the angle of incidence with respect to the flake normal.

In another example, the similarity between an off-plane measurement geometry and several in-plane geometries is investigated. The results are clearly explained when referring to the corresponding values of the flake-based parameters. © 2011 Wiley Periodicals, Inc. *Col Res Appl*, 37, 186–198, 2012; Published online 13 July 2011 in Wiley Online Library (wileyonlinelibrary.com). DOI 10.1002/col.20679

Key words: color measurement; effect coatings; interference pigments; metallic pigments; pearlescent materials

INTRODUCTION

The increasing popularity of effect coatings in markets like automotive and packaging industries is a strong driver for the development of new multi-angle spectrophotometers. For metallic coatings, researchers from AkzoNobel and DuPont established by around 1990 that measurement of the reflection spectra under three different geometries is sufficient to characterize the color travel, i.e., the angular variation of reflectivity.^{1–3} The three geometries should include a wide variation in the so-called aspecular angle, a concept that we will define below. This conclusion has been adopted for example in the ASTM standard for measuring metallic coatings.⁴

In the past 20 years, pigments with more complex coloristic behavior have been introduced in the market, gaining immense popularity as well. Examples include interference (pearlescent) and holographic pigments. For such “special effect pigments,” it has been found that three geometries are no longer sufficient for a full characterization. At least five to six measurement geometries seem to be needed (or even nine according to a recent ASTM norm⁵). The discussion on how many and which geometries are needed is still ongoing.

Over the years, it has become clear that for special effect pigments, the concept of aspecular angle is not sufficient to characterize reflection measurements at different geometries. Therefore in a series of articles, several new concepts were introduced by one of the authors (WRC) in collaboration with investigators from Merck KGaA: cis- and trans- angles, interference lines and aspecular lines.^{6–12} These new concepts were shown to be promising, for example for selecting measurement geometries most suitable for identifying which special effect pig-

*Correspondence to: Eric Kirchner (e-mail: eric.kirchner@akzonobel.com).

TABLE I. Effect pigments covered by the first sample set.

Pigment code	Type of pigment	Color group	Commercial name
A	Metallic—Cornflake (Coarse)	Grey	Stapa Mobilux [®] (Eckart GmbH) R157
B	Metallic—Silver Dollar (Coarse)	Grey	Stapa Metallux [®] (Eckart GmbH) 2153
C	Mica/TiO ₂	Blue	Iriodin [®] 9225 WR Rutile
D	Mica/TiO ₂	Green	Iriodin [®] 9235 WR Rutile
E	Mica/TiO ₂	Lilac	Iriodin [®] 9219 Rutile
F	Mica/Cr ₂ O ₃ /TiO ₂	Green	Iriodin [®] 9444 Moss green WRll
G	Xirallic Al ₂ O ₃ /TiO ₂	Green	Xirallic [®] T60-24 Stellar Green
H	Xirallic Al ₂ O ₃ /TiO ₂	‘White’	Xirallic [®] T60-10 Crystal Silver
I	Colorstream	Violet	Colorstream [®] T20/01 WNT Viola Fantasy
J	Chromaflair	Green	Chromaflair [®] Green Purple 190

ments are present in an unknown material, or for identifying the conventional, absorption pigments in an effect coating. However, the applicability of using these concepts for such goals was never systematically tested in the open literature, and their use is still rather limited.^{13–16}

Because of this unclear status of research, new multi-angle spectrophotometers have been launched with different sets of measurement geometries. Recently, BYK Gardner introduced the BYK-mac[®], that features six measurement geometries including both trans- and cis-geometries. X-Rite introduced the MA98[®] instrument, having 19 different geometries including both trans- and cis-geometries, and also including off-plane geometries. Instruments that are capable of measuring at hundreds or even thousands of different geometries have also become available. These so-called BRDF (Bidirectional Reflectance Distribution Function) measurement devices are currently accessible through for example the Physikalisch-Technische Bundesanstalt in Braunschweig, the National Physical Laboratory (UK), the National Institute of Standards and Technology (US), the Katholieke Universiteit Leuven (Belgium)¹⁷ and Murakami Research (Japan).¹⁸

From a straightforward statistical analysis of BRDF reflection data, Baba and coworkers¹⁸ conclude that 1485 different geometries are required for characterizing the reflection properties of special effect coatings. But storing reflection data for such a large number of geometries, for many thousands of samples, would create serious problems in terms of time and cost efficiency in many industries. A reduction of the number of measurement geometries is only possible with a physical interpretation of the reflectivity at different measurement geometries. This is the goal of this article.

Using a dedicated set of samples in which different types of special effect pigments are included, we investigate the applicability of the currently used concepts: aspecular angles, cis- and trans-geometries, interference lines and aspecular lines. Our goal is to use such concepts to find those geometries for which the largest changes in reflection values can be expected after systematic changes in the pigment, and for finding geometries for which a large similar-

ity between reflection curves should be expected. Apart from the currently used concepts, we also introduce a new concept, which we think is better suited for this goal. These are the so-called flake-based parameters introduced below.

We note that in this article, we will only investigate reflection coefficients and the colorimetric properties derived from them. Additional information on visual appearance, such as the parameters describing visual texture that are also measured by the BYK-mac instrument,^{19,20} are not addressed here. Similarly, none of the mathematical transformations on reflection measurements, proposed by X-Rite for the MA98 instrument, are investigated here.²¹

EXPERIMENTAL

Sample Set

In this investigation, reflection measurements of samples are carried out under many different geometries, using three different instruments. Therefore the number of samples included in the tests had to be limited to around 50. We chose to focus on the 10 different effect pigments listed in Table I. When taken together, they represent a wide range of effect pigments, from metallic pigments via the conventional mica-based interference pigments to the Xirallic[®] (Merck KGaA, Darmstadt, Germany), Colorstream[®] (Merck KGaA, Darmstadt, Germany), and Chromaflair[®] (JDSU Flex Products, Milpitas, USA) pigments, with the resulting large color travel. Where applicable, the pigments were selected such that they belonged to the same color group as much as possible.

Each effect pigment was applied in three different concentration levels, ranging from low to high. For each of these concentration levels, five different concentration ratios of blue and green absorption pigments were tested. This is summarized in Table II. In this way, the medium

TABLE II. Mixtures used in the test, defined as weight concentrations.

Mixture	Effect pigment	Blue absorption pigment	Green absorption pigment
01	50	7.00	0.00
02	50	5.25	1.75
03	50	3.5	3.5
04	50	1.75	5.25
05	50	0.00	7.00
06	20	37.00	0.00
07	20	27.75	9.25
08	20	18.50	18.50
09	20	9.25	9.25
10	20	0.00	37.00
11	07	50.00	0.00
12	07	37.50	12.50
13	07	25.00	25.00
14	07	12.50	37.50
15	07	0.00	50.00

Note that the ratio between the concentrations of blue and green absorption pigments covers the same range for each of the three concentration levels of effect pigment, namely 1:0, 3:1, 1:1, 1:3, and 0:1.

TABLE III. Design of color formulas tested in this study.

Mixture	Effect pigment									
	A	B	C	D	E	F	G	H	I	J
01	L	L		L		L			L	L
02	L	L		L		L		L	L	
03	L	L		L					L	
04	H	H		H		H	H	H	H	H
05	H	H		H		H	H	H	H	H
06	L	L	L		L	L		L	L	L
07	L	L	L	L					L	L
08	L	L		L						L
09										
10	L	L				L	L			
11	L	L				L	L	L		
12							L	L		
13										
14										
15										
Number of samples selected	10	10	2	7	1	7	5	6	7	6

The 10 columns show effect pigment code according to Table I, whereas the 15 rows show mixtures according to Table II. Each of the $10 \times 15 = 150$ resulting mixtures was sprayed out in combination with low (L) and also with high (H) concentration of black absorption pigment. Cells with L or H entries were finally selected for further investigation.

surrounding the effect pigments ranges from pure blue to pure green.

Since the hiding properties of the effect pigments tested here are often poor, and also vary greatly between these pigments, black absorption pigment was added at two different concentration levels (mass concentrations of 2 and 5 percent). Thus the whole design included $10 \times 3 \times 5 \times 2 = 300$ samples.

Each of the samples was sprayed out in fourfold; the sample with best spray quality was used for subsequent analysis. From the resulting samples, several could not be used because they were not hiding. In the end, we made a selection of 61 samples that show good hiding while still representing a wide range of effect pigments. The composition of these samples is clarified in Table III.

In this article, we will refer to the samples according to the data in Tables I–III. For example, sample J06L will refer to the sample with effect pigment Chromaflair Green Purple 190 (the J refers to this pigment according to Table I), from which 20 g of toner is combined with 37.00 g of blue absorption pigment toner (the 06 refers to this mixture, according to Table II), which in turn is combined with a low concentration of black absorption pigment toner (the L label according to Table III).

Instruments and Geometries

In this investigation, we use three different multi-angle spectrophotometers.

- A BYK-mac[®] instrument, commercially available through BYK Gardner. It measures reflections at six different geometries.

- An MA98[®] instrument from X-Rite, measuring reflection values at 19 different geometries, including eight off-plane geometries.
- A GK311/M[®] instrument from Zeiss that is capable of selecting any illumination and detection angle with a step size of 5°. Because of limitations due to sterical hindrance between light source and detector, a total of 220 different measurement geometries are available. To save measurement time, we selected 98 geometries best suitable for the analysis, as listed in Table IV.

For in-plane measurement geometries, we will use the notation prescribed in ASTM norm⁵ E2539-08. This means that illumination angle θ_{ill} and detection angle θ_{det} are both taken with respect to the coating normal. Illumination angles are positive by definition. The angle between detector and the specular direction is referred to as the aspecular angle θ_{aspec} . Its sign is defined by taking the direction from the specular direction toward the coating normal as positive. The notation of measurement geometries is defined by specifying illumination angle and detection angle, separated by a colon. Next, the aspecular angle is enclosed in parenthesis. This notation is illustrated in Fig. 1. In Table V, this notation is used to denote the geometries available in the BYK-mac and the MA98 instruments.

For off-plane measurement geometries, the light source, coating normal, and detector are not part of the same plane. In this case, also the azimuthal angle γ needs to be specified. In our notation, this is always an angle between -90° and $+90^\circ$. A zero value is used for in-plane mea-

TABLE IV. Measurement geometries used with the Zeiss GK/311M spectrophotometer.

Detection angle θ_{det}	Illumination angle θ_{ill}										
	15°	20°	25°	30°	35°	40°	45°	50°	55°	60°	65°
45°											21
40°											20
35°											19
30°											18
25°								64		35	17
20°						75	63		45		16
15°						74	62	51			15
10°					83	73	61		44	34	14
5°			94	89	82	72	60			33	13
0°		97	93	88	81	71	59		43	32	12
-5°	98	96	92	87	80	70	58			31	11
-10°		95	91	86	79	69	57		42	30	10
-15°			90	85	78	68	56	50		29	09
-20°				84	77	67	55		41	28	08
-25°					76	66	54	49	40	27	07
-30°						65	53	48	39	26	06
-35°							52	47	38	25	05
-40°								46	37	24	04
-45°									36	23	03
-50°										22	02
-55°											01

Cell entries show number labeling the geometry. For example, the ZEISS-21 geometry has illumination angle $\theta_{\text{ill}} = 65^\circ$ and detection angle $\theta_{\text{det}} = 45^\circ$.

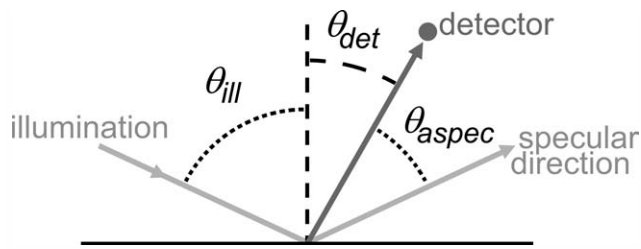


FIG. 1. Notation for in-plane measurement geometries. In this case, the illumination angle $\theta_{ill} = 65^\circ$ whereas the detection angle $\theta_{det} = -30^\circ$. This results in an aspect angle $\theta_{aspec} = +35^\circ$. Hence, according to the ASTM definition this geometry is designated as $65^\circ:-30^\circ$ (as $+35^\circ$).

surement, whereas a positive value is used if the detector has been rotated counter-clockwise from the specular angle toward the light source, as viewed from above. The notation is illustrated in Fig. 2, where it is also compared with the notation that X-Rite uses for its off-plane geometries. The main difference between these two notations is that X-Rite determines azimuthal angles by rotation around the specular direction, whereas in our case the rotation is around the coating normal.

Measurement Procedure

The three spectrophotometers were calibrated in a similar but not totally identical way. White calibration was done using a BCRA tile for the BYK-mac and the MA98, but using an opal sample for the Zeiss instrument. The Zeiss instrument did not require black calibration, whereas a light trap was used for the other two instruments.

A potentially more important difference between the instruments is that for the BYK-mac and the MA98, reflection curves are measured by averaging over four

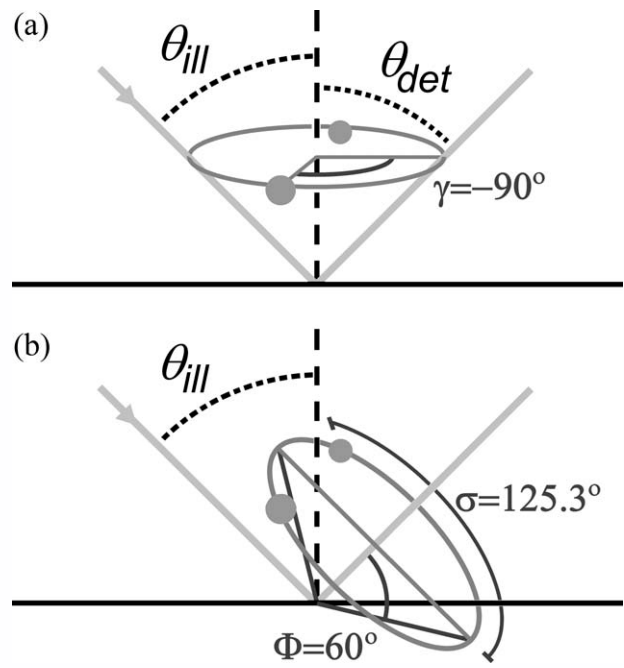


FIG. 2. Notation for off-plane geometries. Green dots refer to positions of the two detectors. The left hand side shows why the azimuthal angle $\gamma = \pm 90^\circ$ for these two geometries, while the right hand side shows why these same geometries are referred to as having azimuthal angle $\pm 125.3^\circ$ in the X-Rite notation. As a consequence, these two measurement geometries are labeled as $45:-45$ (as 60 , azimuthal $\pm 90^\circ$) here, and $45as60az \pm 125.3$ by X-Rite.

sample rotations. This is done to reduce the effect of dust and nonisotropic flake orientation distributions, and leads to more stable measurement data. However, to save time the measurements with the Zeiss instrument involve measurements under a single panel orientation. Another difference between the three instruments is the diameter of the

TABLE V. Measurement geometries for the BYK-mac and MA98.

BYK-mac and/or MA98 geometry	Illumination angle θ_{ill}	Detection angle θ_{det}	Aspect angle θ_{aspec}	Azimuthal angle θ	Flake orientation angle θ_{flake}	Flake-angle of incidence θ_{inc}
BM_01: -15°; MA98_01: 45as-15	45°	-60°	-15°		3.6°	31.7°
BM_02: $+15^\circ$; MA98_02: 45as15	45°	-30°	15°		-4.3°	23.8°
BM_03: 25°; MA98_03: 45as25	45°	-20°	25°		-7.5°	20.7°
BM_04: 45°; MA98_04: 45as45	45°	0°	45°		14.1°	14.1°
BM_05: 75°; MA98_05: 45as75	45°	30°	75°		23.8°	4.3°
BM_06: 110°; MA98_06: 45as110	45°	65°	110°		32.6°	-4.5°
MA98_07: 15as-15az0	15°	-30°	-15°		4.8°	14.7°
MA98_08: 15as15az0	15°	0°	15°		5.0°	5.0°
MA98_09: 45as25az90	45°	-50.1°	25°	33.4°	9.3°	28.1°
MA98_10: 45as25az-90	45°	-50.1°	25°	-33.4°	9.3°	28.1°
MA98_11: 45as60az125.3	45°	-45°	60°	90°	20.7°	19.5°
MA98_12: 45as60az-125.3	45°	-45°	60°	-90°	20.7°	19.5°
MA98_13: 15as-45	15°	-60°	-45°		12.7°	22.6°
MA98_14: 15as45	15°	30°	45°		14.7°	-4.8°
MA98_15: 15as80	15°	65°	80°		23.6°	-13.6°
MA98_16: 15as38.3az43	15°	-50.1°	38.3°	33.4°	11.6°	19.7°
MA98_17: 15as38.3az-43	15°	-50.1°	38.3°	-33.4°	11.6°	19.7°
MA98_18: 15as46.9az104.5	15°	-45°	46.9°	90°	15.1°	14.8°
MA98_19: 15as46.9az-104.5	15°	-45°	46.9°	-90°	15.1°	14.8°

Angles as defined in the text. The last two columns show parameters defined in later sections of the text.

measurement spot, which is 20 mm for the BYK-mac, 12 mm for the Zeiss instrument and 15 mm for the MA98.

Further, for reasons of simplicity, the difference in reflection curves measured under different measurement geometries is expressed as ΔE_{ab}^* .

RESULTS

Cis- versus Trans-Geometries

Above, we have already introduced the term aspecular angle describing the angular difference between detector and specular angle. In a number of articles, one of the authors (WRC) together with researchers from Merck KGaA introduced several new concepts for describing the angular dependence of reflection curves for special effect coatings.^{6–12}

Instead of using only the aspecular angle as an absolute number, it was demonstrated that the sign of this number is important as well. Measurement geometries with a negative aspecular angle in Table V are now referred to as trans-geometries, whereas positive aspecular angles are labeled as cis-geometries.^{8,11} Our measurements with the BYK-mac instrument confirm the distinction between these two situations. The average color difference between reflection curves measured at the trans -15° geometry and those measured at the cis $+15^\circ$ geometry is $\Delta E_{ab}^* = 14.7$. This shows that indeed these two geometries often lead to different reflection measurements.

Interestingly, samples containing metallic pigments and samples containing mica-based effect pigments show a smaller difference, with an average $\Delta E_{ab}^* = 10.8$ and 6.2 , respectively. Samples containing Xirallic pigments show an average of $\Delta E_{ab}^* = 6.9$. However, the average difference between reflection curves for the cis- and trans-geometry are $\Delta E_{ab}^* = 37.7$ for samples containing Colorstream or Chromaflair pigments. Apparently, the latter effect pigments lead to very large differences between cis- and trans-geometries.

Comparing the reflection curves, for metallic samples the reflection values measured at the trans -15° geometry are primarily shifted to larger reflection values when compared with those measured at the cis $+15^\circ$ geometry, resulting mainly in an increase in lightness. For samples containing mica-based effect pigments, or the “white” Xirallic Crystal Silver pigment, no such increase in reflection value or lightness is observed. Instead, we find a small shift in reflection curve toward shorter wavelengths, over less than 5 nm, affecting mainly the hue. A similar wavelength shift, but often over a substantially larger range of wavelengths (depending on coating composition), is found for samples that contain pigments such as Colorstream, Chromaflair, and colored Xirallic pigment.

Practical results like this show the added value of using the concept of cis- versus trans-geometries instead of only aspecular angle, especially when investigating colored effect pigments with large color travel. However, up to date no clear physical explanation was given why these concepts make sense. We will come back to this topic below.

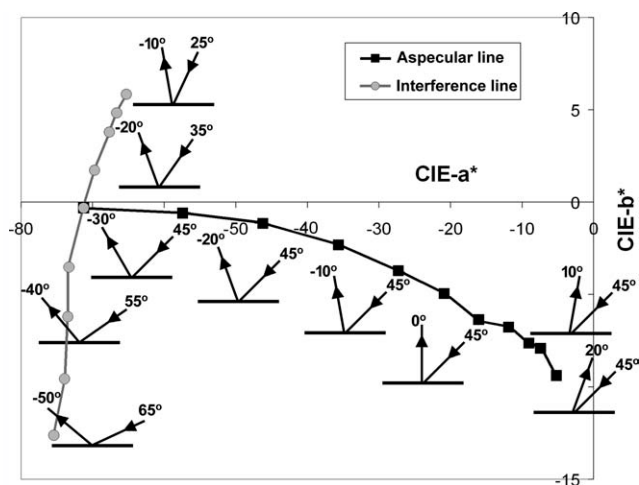


FIG. 3. Illustration showing an aspecular line (with θ_{ill} fixed at 45°) and an interference line (with θ_{aspec} fixed at 15°). The data in this example were measured for a mixture of interference pigment Iriodin[®] (Flex Products) 9444 Moss green WR11, mixed with blue absorption pigment and a low concentration of black absorption pigment (sample F01L).

Interference Lines and Aspecular Lines

As a result of practical experience, the studies cited above also introduced the concepts of interference lines and aspecular lines. Interference lines connect the color coordinates obtained from a series of measurement geometries that have a fixed value for the aspecular angle. Similarly, aspecular lines (sometimes called “Glanzlinien” in German) are defined by series of measurement geometries with the same value for the illumination angle. An example of an interference line and an aspecular line is shown in Fig. 3.

Considering interference lines and aspecular lines, three different claims have been brought forward in previous work.

First Claim: “Interference Lines Characterize Effect Pigments”

It has been claimed in earlier publications that interference lines, especially those with an aspecular angle of 25° or less, can be used to recognize which special effect pigments are present in an effect coating.^{7,8} This claim was confirmed for the samples studied here. As an example, Fig. 4(a) shows interference lines with a fixed aspecular angle of 15° for six different samples. Three of these samples contain pigment Chromaflair Green Purple 190 (mixed with different combinations of absorption pigments and in different concentrations of effect pigment), and similarly the three other samples contain Colorstream pigment. It is clear from Fig. 4(a) that the shape of the interference line for these two effect pigments is very distinct, and indeed might be useful for recognizing the type of effect pigment in an unknown coating, independent of the concentration of the effect pigment and/or combination of absorption pigments.

However, our results indicate that this potential for recognizing effect pigments is limited to colored effect pig-

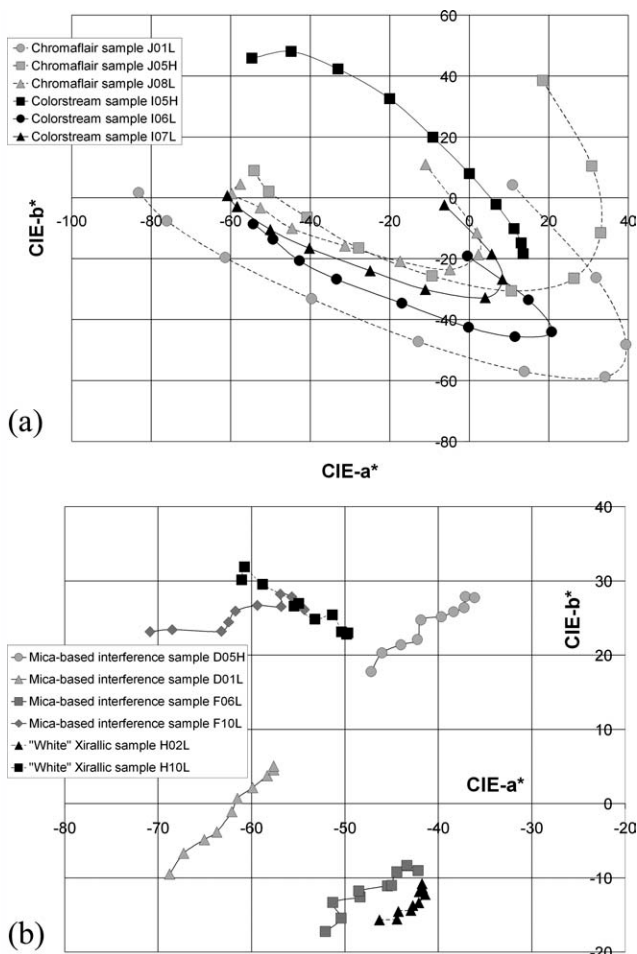


FIG. 4. Interference lines for an aspecular angle of 15° , for samples containing (a) Chromaflair and Colorstream effect pigment, (b) two different mica-based interference pigments and “white” Xirallic pigment.

ments with large color travel, like Chromaflair, Colorstream, and colored Xirallic pigments. For effect pigments that have a much smaller color travel, such as mica-based interference pigments and Xirallic Crystal Silver pigment, interference lines are much shorter and less characteristic. This is illustrated in Fig. 4(b), where the difference in scale with Fig. 4(a) should be noted. It is clear from Fig. 4(b), that the interference line alone cannot be considered as a good tool to distinguish between different mica-based interference pigments or Xirallic Crystal Silver pigment. In this respect, Xirallic Crystal Silver pigment behaves more like metallic pigments. A more promising approach to characterize the appearance of coatings containing this pigment is to measure texture parameters, thus attempting to capture the pigment’s “living sparkle.”²²

Second Claim: “Interference Lines and Aspecular Lines Run Parallel for Metallic Samples”

It has also been claimed that interference lines and aspecular lines run parallel for metallic samples but not for samples containing other effect pigments.⁸ As a gen-

eral rule, this claim was also confirmed by the samples studied here. As an example, Fig. 5(a) shows an interference line and an aspecular line for two samples. For sample B05H, which contains metallic pigment, the two lines run parallel indeed. But for sample D04H, which contains a mica-based interference pigment, this is not the case, as predicted by the rule.

The rule was found to be valid for most of our samples. An exception occurs again for some of the panels that contain pigment Xirallic T60-10 Crystal Silver, such as sample H05H. Figure 5(b) shows that for this sample the interference line and aspecular line unexpectedly run parallel. On the other hand, the same figure shows that sample H02L, containing the same pigment, does follow the general rule. None of the samples containing pigment Xirallic T60-24 Stellar Green shows the anomalous behavior. Apparently, it is only the “white” pigment Xirallic T60-10 Crystal Silver that may behave more or less like a metallic pigment. This result is in line with the results obtained above.

Figure 5(b) also shows the results for sample A02L. Although the sample contains a metallic effect pigment,

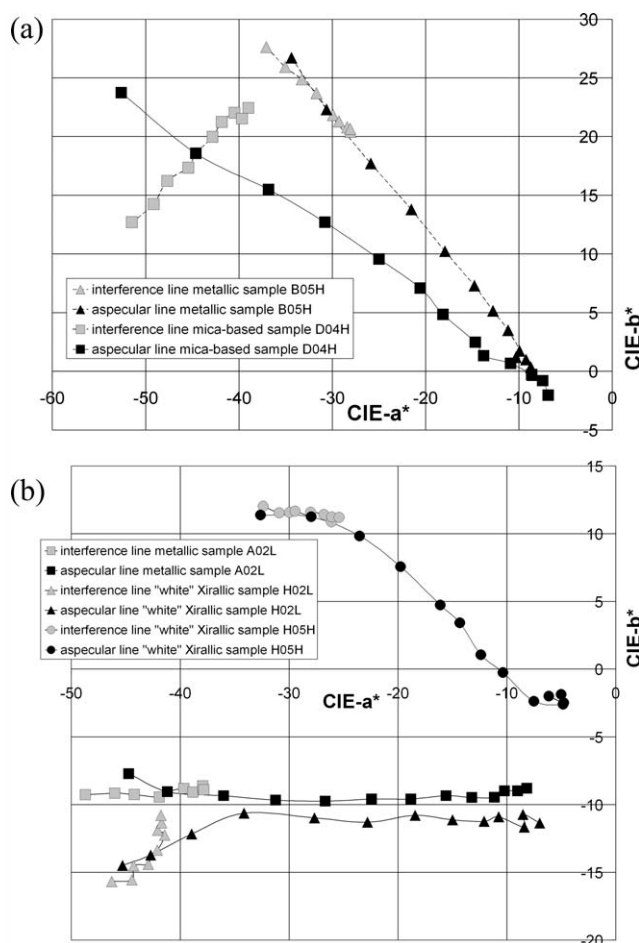


FIG. 5. Interference lines (for aspecular angle fixed at 15°) and aspecular lines (for illumination angle fixed at 45°). (a) Two samples that follow the general rule, containing a metallic and a mica-based interference pigment. (b) Three examples, from which two do not follow the general rule. These examples contain a metallic and Xirallic pigment.

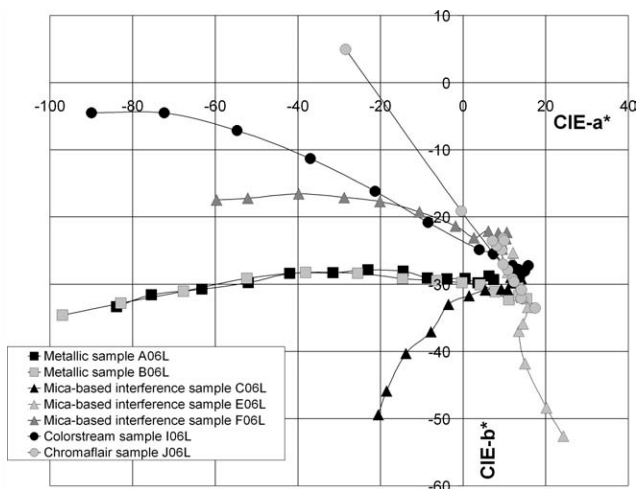


FIG. 6. Aspecular lines (for illumination angle fixed at 25°) for seven samples containing the same blue combination of absorption pigments, but containing different effect pigments. For large aspecular angle, all measurements are seen to converge to the blue area of color space.

the interference line and aspecular line do not run completely parallel. Based on Fig. 5(b), it does not seem to be possible to use the claimed rule for recognizing which measurement data refer to a metallic sample, and which refer to a Xirallic pigment.

In conclusion, our results show that the second claim is confirmed as a general rule, but that exceptions to it do occur, for example for “white” effect pigments such as Xirallic T60-10 Crystal Silver.

Third Claim: “Aspecular Lines Characterize Mainly Scattering by Absorption Pigments”

It has been claimed that aspecular lines contain mainly contributions from scattering by absorption pigments (as opposed to contributions from flake reflection).⁷ To test if this claim is confirmed in our set of samples, we have taken seven different samples that contain different effect pigments, but each of which contains exactly the same amounts and types of absorption pigments. If the claim is correct, the resulting aspecular lines should be identical.

The results in Fig. 6 show that in this form, the claim is not confirmed by our data. When mixed with different effect pigments, the same amounts and combination of absorption pigments yield different aspecular lines.

On the other hand, Fig. 6 also shows that the focal point of these aspecular lines may be the same. When extrapolating the lines in Fig. 6, it appears that they more or less converge to the same focal point (or focal area). This focal point would represent the color coordinates for a measurement geometry with maximum aspecular angle, (much) larger than the 110° included in this study.

We did not further investigate if adding such an extremely high aspecular angle to the available geometries in a spectrophotometer can indeed be useful for recognizing the absorption pigments in an effect coating.

This option is interesting, and is in fact independent of the use of aspecular (and interference) lines.

INTERPRETATION OF RESULTS

In the previous section, we discussed several claims that have been made about the coloristic behavior of effect coatings. These claims have been proposed based on practical experience but still lack physical explanation. Although most claims were confirmed by our data, for the third claim this was not the case. Moreover, exceptions were found to the first two claims. Therefore, a more physical approach to interpreting measurement geometries is needed.

We will propose here such a new approach, based on so-called flake-based parameters. It will be introduced below. This will be followed by the interpretation that it offers for the confirmations and nonconfirmations of the claims discussed above. Finally, we will discuss how the new approach may help to interpret reflection data obtained at other geometries, such as the off-plane geometries of the MA98 instrument.

Introducing Flake-Based Parameters

Up to now, we have designated measurement geometries according to the angles of illumination and detection with respect to the coating surface. As a quantity derived from these two angles, also the aspecular angle is implicitly defined with respect to a coordinate system fixed by the coating surface. Such a notation is convenient, since angles with respect to the coating surface are easily measured.

However, for effect coatings the essential physics does not take place at the surface of the coating, but inside the coating, in the interference layers of the effect particles (flakes). From a physical point of view, the measurement geometry is therefore better expressed in terms of the angle of incidence with respect to the normal vector of the flakes.

Obviously, this presents a difficulty, because the pigment flakes in an effect coating do not all have the same orientation. Instead, their orientation follows a distribution that depends on flake type, concentration, etc.²³

To be able to account for flake orientation, we assume that light reaching the detector necessarily was reflected from a flake which had exactly the right orientation to deflect light, originating from the direction of the light source, toward the direction of the detector. All light that encounters a flake with a different orientation is assumed to be reflected to directions not signaled by the detector.

We remark that this approach ignores the fact that light may experience multiple reflection from flakes, or that it may be scattered from conventional absorption pigments. Therefore, our approach may be expected to be less valid for geometries with a large value of the aspecular angle, since for those geometries multiple flake reflection and/or scattering by absorption pigments may be substantial.

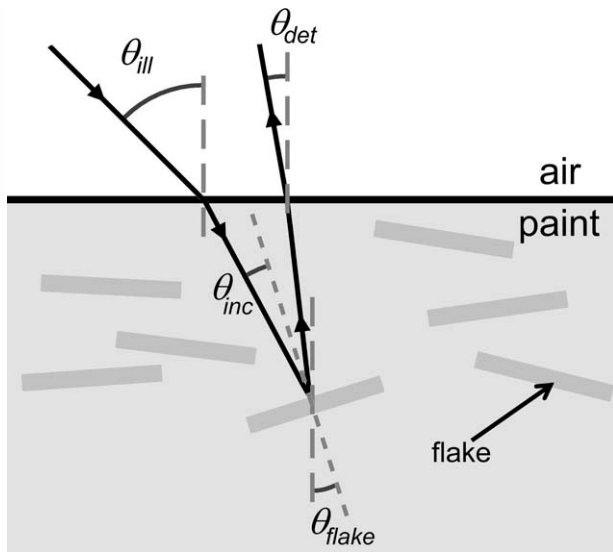


FIG. 7. Illustration of the meaning of the flake-based parameters. The parameter θ_{flake} describes the flake orientation angle of those flakes that reflect light, originating from the light source, directly in the direction of the detector or the observer. The parameter θ_{inc} refers to the angle of light incidence, with respect to the flake normal. Both parameters are calculated by accounting for the refractive index of the coating medium.

The mathematical analysis needed to define flake-based angles is straightforward. We will assume that the refractive index of the coating is 1.5, which is correct for most coatings. Taking the conventional definitions of illumination angle θ_{ill} and detection angle θ_{det} as defined with respect to the coating normal, Snellius' law allows us to calculate the exact value for the flake disorientation angle θ_{flake} that directly deflects light exactly from the light source toward the detector. This is illustrated in Fig. 7.

Limiting ourselves to in-plane geometries we find:

$$\theta_{flake} = \pm \frac{1}{2} \left(\arcsin \left[\frac{n_{air}}{n_{coat}} \sin \theta_{det} \right] + \arcsin \left[\frac{n_{air}}{n_{coat}} \sin \theta_{ill} \right] \right) \quad (1)$$

where the sign is positive in case light source and detector are positioned at the same side of the coating normal, and negative when they are at opposite sides.

Further, the angle of incidence θ_{inc} of the light with respect to the flake normal is calculated as:

$$\theta_{inc} = \frac{1}{2} \left(-\arcsin \left[\frac{n_{air}}{n_{coat}} \sin \theta_{det} \right] + \arcsin \left[\frac{n_{air}}{n_{coat}} \sin \theta_{ill} \right] \right) \quad (2)$$

Obviously, the amount of interference and/or absorption by a flake pigment depends only on the angle of incidence θ_{inc} , calculated with respect to the flake normal. Therefore this parameter is better qualified for recognizing the type of effect pigment than the conventionally used illumination angle θ_{ill} and detection angle θ_{det} . We note here that in a draft norm of the ASTM E12.12 committee WK1164, a similar idea was developed under the name of "color angle."²⁴ Unfortunately, this idea was

only hinted at in a draft version of the norm. In the draft, the idea was not worked out (for example, it did not yet take into account Snellius' law). In the final version of the norm, the idea was abandoned altogether.⁵

Given the values of the conventionally used illumination angle θ_{ill} and detection angle θ_{det} , the corresponding values for θ_{flake} and θ_{inc} are easily calculated with these equations. For the measurement geometries in the BYK-mac and MA98, the resulting values are included in Table V.

For off-plane geometries, a similar derivation leads to the following expressions:

$$\cos \theta_{flake} = \frac{\cos \theta_1 + \cos \theta_2}{[2 + 2 \sin \theta_1 \sin \theta_2 \cos \phi_{out} + 2 \cos \theta_1 \cos \theta_2]^{1/2}}$$

$$\cos(2\theta_{inc}) = \sin \theta_1 \sin \theta_2 \cos \phi_{out} + \cos \theta_1 \cos \theta_2$$

where the parameters θ_1 , θ_2 and ϕ_{out} are calculated from

$$n_{air} \sin \theta_{ill} = n_{coat} \sin \theta_1$$

$$n_{air} \sin |\theta_{det}| = n_{coat} \sin \theta_2$$

$\phi_{out} = 180^\circ + \gamma$ for off-plane geometries, while for in-plane geometries $\phi_{out} = 0^\circ$ if light source and detector are at the same side of the coating normal, and $\phi_{out} = 180^\circ$ if they are at opposite sides of the coating normal. A document showing the full derivation of these equations is available from the corresponding author.

USING FLAKE-BASED PARAMETERS FOR INTERPRETING OBSERVED TRENDS

Claim: "Interference Lines and Aspecular Lines Run Parallel for Metallic Samples"

Above, we confirmed the claim that for metallic samples, the aspecular lines and interference lines run parallel, and that this is not the case for samples containing colored special effect pigments. This trend was found based on experience with effect coatings, but it was not clearly explained in terms of the physics. Using the flake-based parameters, however, this trend is easy to explain.

For metallic pigments, the flake reflection value does not depend on the angle of incidence θ_{inc} , calculated with respect to the local flake normal. Therefore the reflection curve of a coating sample, measured for a particular measurement geometry, only depends on the value of the parameter θ_{flake} . Starting from a measurement geometry, we can change the detection angle (as is done for generating an aspecular line), or we can change the illumination and detection angle simultaneously by keeping the aspecular angle fixed (as is done for generating an interference line). But these changes are only important as far as they lead to changes in the parameter θ_{flake} , and therefore are one dimensional in character. Hence, the resulting change in color space is along a single line, making the aspecular line and interference line to run parallel. This is indeed what is found experimentally, as exemplified for the metallic sample shown in Fig. 5(a).

TABLE VI. Angular data for interference line with aspecular angle fixed at 15°.

Illumination angle θ_{ill}	Detection angle θ_{det}	Aspecular angle θ_{aspec}	Flake orientation angle θ_{flake}	Flake-angle of incidence θ_{inc}
35°	-20°	15°	-4.7°	17.8°
40°	-25°	15°	-4.5°	20.9°
45°	-30°	15°	-4.3°	23.8°
50°	-35°	15°	-4.1°	26.6°
55°	-40°	15°	-3.9°	29.2°

So when examining the color coordinates of metallic samples for different measurement geometries, only the value of the parameter θ_{flake} is important. When this value increases, flakes are addressed with a larger disorientation angle. Since flake orientation distributions are usually peaked at horizontal orientation, with flakes lying parallel to the coating surface,²³ this corresponds to measurement geometries for which the path length of light is more subjected to the absorption pigments in the coating. Measurement geometries with smaller values of the θ_{flake} parameter result in reflection curves that are less strongly affected by absorption pigments.

These conclusions are also expected to be valid for the Xirallic Crystal Silver pigment. Its “white” appearance indicates that the flake reflectivity does not depend on the angle of incidence with respect to the flake normal just like the case for metallic pigments. Indeed, our measurements show the similarity in behavior between Xirallic Crystal Silver pigment and metallic pigments [cf. Fig. 5(b)].

For more strongly colored effect pigments, such as Colorstream, Chromaflair, and colored Xirallic pigments, the flake reflection value does also change with the local angle of incidence θ_{inc} . Hence, changing the measurement geometry leads to a two-dimensional change in color space, and the aspecular line and interference line no longer run parallel.

This indeed summarizes and explains most of the observed trends.

Claim: “Interference Lines Characterize Effect Pigments”

We have seen that our results confirm the claim that interference lines are particularly suitable for characterizing the angular variation in reflectance properties of effect pigments. We found that this is the case especially for colored effect pigments with large color travel, like Chromaflair, Colorstream, and colored Xirallic pigment. The claimed behavior does not seem to be valid for samples that contain metallics, mica-based interference pigments or the “white” Xirallic Crystal Silver pigment.

In Table VI, we see that a series of measurement geometries following an interference line corresponds to keeping the parameter θ_{flake} quite constant, while varying the angle of incidence θ_{inc} , calculated with respect to the local flake normal. This explains why the interference line characterizes effect pigments: it samples the reflectance

value of flakes as a function of the angle of incidence with respect to the flake normal.

In conventional procedures for the visual assessment of effect coatings, light source and observer are kept at the same place while the sample is rotated. This results in a series of geometries like those on the aspecular line mentioned in Table VII. In such a series, both parameters θ_{flake} and θ_{inc} are varied simultaneously. As a consequence, no clear characterization of the reflectance properties of the effect pigment is possible. In fact, this also explains why we found no confirmation for the third claim, stating that aspecular lines could be used to characterize scattering by noneffect pigments. Since along an aspecular line both flake-based parameters are varied, the varying contributions from absorption pigments cannot be distinguished from those from effect pigments.

Hence the concept of flake-based angles allows us to understand the applicability of interference lines and the more problematic applicability of aspecular lines in characterizing effect pigments. It also explains why interference lines for “white” Xirallic Crystal Silver pigments and the weakly colored mica-based interference pigments are short. For those pigments, the reflection coefficient of the pigment particle itself has only a weak dependence on the angle of incidence at the flake.

In fact, from these results it is possible to improve the explanatory power of interference lines, thus better characterizing effect pigments. For example, in the interference line with a fixed aspecular angle of 15°, the current definition includes both the ($\theta_{\text{ill}} = 45^\circ$, $\theta_{\text{det}} = -30^\circ$) geometry and the ($\theta_{\text{ill}} = 65^\circ$, $\theta_{\text{det}} = -50^\circ$) geometry. However, these two geometries have quite different values for θ_{flake} , namely -4.3° and -3.2°, respectively. Instead of the latter geometry it would be better to include the ($\theta_{\text{ill}} = 65^\circ$, $\theta_{\text{det}} = -45^\circ$) geometry, since it corresponds to the same value of θ_{flake} as the ($\theta_{\text{ill}} = 45^\circ$, $\theta_{\text{det}} = -30^\circ$) geometry. We will come back to this example in a next section.

Similarity Between Measurement Geometries

For the following analyses, it is useful to define a parameter that quantifies to what extent reflection curves measured under two different geometries are different. This parameter will be called the dissimilarity index. It is calculated by taking the color difference between the reflection curves. For the sake of simplicity, the CIELAB ΔE_{ab}^* value will be used instead of more advanced color

TABLE VII. Angular data for aspecular line with illumination angle fixed at 45°.

Illumination angle θ_{ill}	Detection angle θ_{det}	Aspecular angle θ_{aspec}	Flake orientation angle θ_{flake}	Flake-angle of incidence θ_{inc}
45°	-20°	25°	-7.5°	20.7°
45°	-25°	20°	-5.9°	22.2°
45°	-30°	15°	-4.3°	23.8°
45°	-35°	10°	-2.8°	25.3°
45°	-40°	5°	-1.4°	26.7°

TABLE VIII. Angular data for several geometries investigated with the Zeiss GK/311M instrument.

Geometry	Illumination angle θ_{ill}	Detection angle θ_{det}	Aspecular angle θ_{aspec}	Flake orientation angle θ_{flake}	Flake-angle of incidence θ_{inc}	Dissimilarity index (ΔE_{ab}^*)
Zeiss-53	45°	-30°	15°	-4.3°	23.8°	0.0
Zeiss-66	40°	-25°	15°	-4.5°	20.9°	6.5
Zeiss-47	50°	-35°	15°	-4.1°	26.6°	6.5
Zeiss-03	65°	-45°	20°	-4.5°	32.6°	13.1

The last column shows the value of the dissimilarity index (derived in the main text), calculated between each measurement geometry and geometry Zeiss-53.

difference equations, since no connection with a visually perceived color difference is strived for. The value of the dissimilarity index between two measurement geometries is then taken to be the average ΔE_{ab}^* of the 61 samples in the sample set.

In some cases, it is useful to also look at specified selections of samples. For example, the averaging may be carried out over the metallic samples in the set.

As a first example, we investigate the cis +15° geometry that is present in the BYK-mac instrument and in the MA98 instrument. This measurement geometry was also included in the geometries we tested with the Zeiss instrument: Table IV shows that indeed the Zeiss-53 geometry has $\theta_{\text{ill}} = 45^\circ$ and $\theta_{\text{det}} = -30^\circ$. The dissimilarity index between the Zeiss-53 geometry and each of the other Zeiss geometries from Table IV is calculated and shown in Table VIII.

In this way, we found that geometries Zeiss-66 and Zeiss-47 are most similar to the Zeiss-53 geometry. Referring to Table IV, this is no surprise. The geometries Zeiss-66 and Zeiss-47 have a cis +15° geometry, just like the Zeiss-53 reference geometry. They are related to the Zeiss-53 geometry by simply decreasing (respectively, increasing) the angle of illumination by 5°. In terms of the flake-based parameters, the high similarity of geometries Zeiss-66 and Zeiss-47 with geometry Zeiss-53 is also understandable, since the corresponding values of parameters θ_{flake} and θ_{inc} are very similar (Table VIII).

The similarity between geometries Zeiss-66 and Zeiss-47 with geometry Zeiss-53 is in fact so good, that the average ΔE_{ab}^* value of 6.5 in both cases is even smaller than the average ΔE_{ab}^* value of 8.1 which is found when comparing geometry Zeiss-53 with the cis +15° geometry of the BYK-mac instrument, or the average ΔE_{ab}^* value of 8.6 which is found when comparing it with the cis +15° geometry of the MA98 instrument. This is remarkable, since those instruments measure under exactly the same measurement geometry as the Zeiss-53 geometry. However, apparently reflection readings from different instruments using the same geometry show a larger mutual difference than reflection measurements from the same instrument at slightly different measurement geometries. This is probably caused by differences in the optical design between the instruments and possibly also by the slightly different calibration procedures that we applied for them.

If we calculate the dissimilarity index by averaging over metallic samples only, we find that geometries Zeiss-66 and Zeiss-47 still show a large similarity with geome-

try Zeiss-53. However, in this case there is one other geometry that shows even more similarity. This is geometry Zeiss-03. Compared with the Zeiss-53 geometry, it has an average color difference for metallic samples of only $\Delta E_{\text{ab}}^* = 2.7$. From the point of view of the traditionally used parameters θ_{ill} , θ_{det} this is unexpected, because geometry Zeiss-03 has $\theta_{\text{ill}} = 65^\circ$ and $\theta_{\text{det}} = -45^\circ$. This would not indicate its best similarity with geometry Zeiss-53, which has $\theta_{\text{ill}} = 45^\circ$ and $\theta_{\text{det}} = -30^\circ$. The aspecular angle of the Zeiss-03 geometry is 20°, so in a naive approach it is not expected to be the geometry most similar to geometry Zeiss-53, that has an aspecular angle of 15°. In terms of the flake-based parameters, the results are easily understood. We have already seen that for metallic samples, only the parameter θ_{flake} is of importance. For that parameter, geometry Zeiss-03 is as similar to geometry Zeiss-53 as are geometries Zeiss-66 and Zeiss-47. Table VIII shows that the corresponding values are $\theta_{\text{flake}} = -4.5^\circ$, -4.3° , -4.5° , and -4.1° , respectively.

Cis- versus Trans-Geometries

Let us now use the concept of flake-based parameters for a further discussion of the results that we found for cis- and trans-geometries. Using the data in Table V, we realize that the trans-15° geometry of the BYK-mac (or the 45as-15 geometry of the MA98) corresponds to a flake disorientation angle $\theta_{\text{flake}} = 3.6^\circ$ and an angle of incidence with respect to the flake normal of $\theta_{\text{inc}} = 31.7^\circ$. For the cis+15° geometry of the BYK-mac (or the 45as+15 geometry of the MA98) the corresponding numbers are $\theta_{\text{flake}} = -4.3^\circ$ and $\theta_{\text{inc}} = 23.8^\circ$.

The sign of the parameter θ_{flake} is not relevant for interpreting the measurements with the BYK-mac and MA98, because these measurements were the result of averaging after four rotations of each sample (see experimental section). Therefore, the flake orientations that are sampled with the trans-15° and the cis+15° geometry are very similar. But the large difference in the value of θ_{inc} for these two geometries shows that in the trans-15° geometry, light is incident on the flakes from a significantly larger angle with respect to their normal vectors than in the case of the cis+15° geometry. This gives a physical explanation why we found clearly different reflection curves for these two measurement geometries in the case of colored effect pigments with large color travel, while we found quite similar reflection curves in the case of

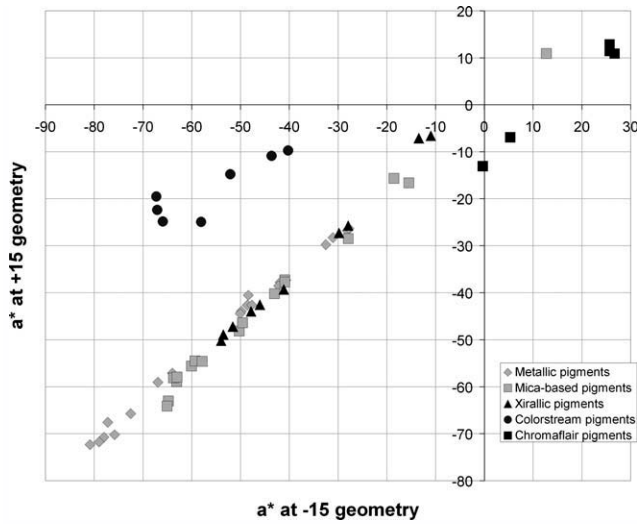


FIG. 8. Correlation between measurements at the -15° and $+15^\circ$ geometry of the BYK-mac instrument, for all samples included in this investigation. A distinction has been made between samples containing different types of effect pigments: Metallics, Mica-based interference flakes, Xirallic, Colorstream, and Chromaflair pigments.

metallic pigments. For metallic pigments, the reflection value of a flake hardly depends on the local angle of incidence. For colored interference pigments with large color travel, such as Colorstream and Chromaflair pigments, this dependence is much stronger because interference effects strongly depend on the local angle of incidence.

This is confirmed by investigating the agreement between colorimetric parameters measured at the trans- 15° and those measured at the cis- $+15^\circ$ geometry. Figure 8 illustrates that for example the values for the CIE a^* coordinate for these two geometries are almost equal for all samples, except for the samples containing the interference pigments Colorstream or Chromaflair (another example of this can be found in Fig. 7 of Ref. 20).

This result shows that in instruments like the BYK-mac and the MA98, the added value of the trans- 15° geometry as an addition to the cis- $+15^\circ$ geometry is probably small for the majority of current automotive colors. But when investigating specifically colored effect coatings with large color travel, the trans- 15° geometry will give distinctive information that should be useful for recognition of effect pigments and/or for color matching.

Another example of the applicability of flake-based parameters is when we investigate the 15as-15az0 geometry of the MA98 instrument. It is a trans- 15° geometry. Therefore, when using only concepts like aspecular angle and cis- and trans-geometries, we might expect this geometry to be more similar to the trans- 15° geometry 45as-15 than to the cis- $+15^\circ$ geometry 45as+15.

However, the measurements show that the opposite is true. The dissimilarity index of the 15as-15az0 geometry with the 45as-15 geometry is $\Delta E_{ab}^* = 26.5$, while with the 45as+15 it is $\Delta E_{ab}^* = 12.0$. This result, which is unexpected when using conventional concepts, can be understood by looking up the values of the relevant flake-based parameters in Table V. In terms of both the θ_{flake} and the θ_{inc} parameter, the 45as+15 geometry is indeed expected to be most similar to the 15as-15az0 geometry.

Off-Plane Geometries

Also for the interpretation of reflections measured at off-plane geometries, flake-based parameters are helpful. As an example, we have calculated the dissimilarity index between the off-plane geometry 45as25az90 of the MA98 instrument and all 98 geometries that we tested for the Zeiss instrument. By sorting the Zeiss geometries according to the value of the dissimilarity index, Table IX is obtained.

Without using flake-based parameters, it would be impossible to understand the results shown in this table. For example, it might be expected that the 45as25az90 of the MA98 instrument shows closest similarity to geometry Zeiss-55, because these geometries are equal in aspecular angle and illumination angle. But a naive analysis like this does not take into account the off-plane character of the 45as25az90 geometry. However, even realizing this it is far from obvious how this off-plane character can be accounted for.

Table IX shows that when using the flake-based parameters θ_{flake} and θ_{inc} , it becomes clear why geometry Zeiss-55 does not show a small dissimilarity index to the 45as25az90 geometry. It also becomes clear then, why instead geometry Zeiss-06 is very similar to the 45as25az90 geometry. Unlike the Zeiss-55 geometry, the Zeiss-06 geometry differs greatly in terms of illumination angle, detection angle and aspecular angle with the 45as25az90 of the MA98 instrument, but it is a close

TABLE IX. Geometries of the Zeiss GK/311M instrument, sorted by the value of their dissimilarity index with the off-plane geometry 45as25az90 of the MA98 instrument.

Geometry	Dissimilarity index (ΔE_{ab}^*)	Illumination angle θ_{ill}	Detection Angle θ_{det}	Aspecular angle θ_{aspec}	Flake orientation angle θ_{flake}	Flake-angle of incidence θ_{inc}
45as25az90	0.0	45°	-50.1°	25°	9.3°	28.1°
Zeiss-06	3.0	65°	-30°	35°	-8.9°	28.3°
Zeiss-27	4.6	60°	-25°	35°	-9.4°	25.8°
Zeiss-40	6.0	55°	-25°	30°	-8.4°	24.7°
Zeiss-56	7.5	45°	-15°	30°	-9.1°	19.0°
Zeiss-55	13.7	45°	-20°	25°	-7.5°	20.7°

match in terms of the parameters θ_{flake} and θ_{inc} . We note that, like before, only the absolute value of θ_{flake} needs to be considered for these measurements.

These results indicate how for any off-plane geometry, the corresponding in-plane geometry can be found with the closest similarity. Since the reflections measured at these geometries will be close but not exactly the same (as quantified by the average value of $\Delta E_{\text{ab}}^* = 3.0$ in the present example), it still remains to be seen what the added value is of off-plane geometries over in-plane geometries.

CONCLUSIONS

Using a sample set prepared dedicated for this study, we tested the validity of several claims related to the use of different measurement geometries for effect coatings.

The claimed added value of using a trans geometry like the -15° geometry in the BYK-mac instrument next to a cis geometry like the $+15^\circ$ geometry in the same instrument, was confirmed. However, it was shown that this added value is expected to be small for samples containing metallic pigments or mica-based effect pigments. It is expected to be large only for colored effect pigments with large color travel, like Colorstream, Chromaflair, and colored Xirallic pigment.

Using the newly proposed concept of flake-based parameters, this limitation in the applicability of the claim could be explained well in terms of the physics involved. Geometries that involve different angles of incidence with respect to the normal vector to the flakes were shown to be responsible for the observed trends.

The claimed potential of interference lines for recognizing effect pigments in an effect coating was confirmed, especially for effect pigments with large color travel. For metallic pigments, mica-based pigments and “white” Xirallic Crystal Silver pigments the claimed characterization was shown to be not very useful. The suggestion that for metallic coatings, interference lines run parallel to aspecular lines whereas this is not the case for other effect pigments was largely confirmed. These results could be physically explained as well. The analysis with flake-based parameters also explains why we found that for the “white” Xirallic Crystal Silver pigment, the claimed behavior was not confirmed.

It has been suggested that aspecular lines can be used to characterize absorption pigments in effect coatings. This suggestion was shown not to be valid based on our measurements, and this result was physically explained by reference to the flake-based parameters.

The concept of flake-based angles allows us to understand the applicability of interference lines and the more problematic applicability of aspecular lines in characterizing the reflectance properties of effect pigments. Interference lines are suitable for characterizing effect pigments because they sample the reflectance values of flakes as a function of the angle of incidence with respect to the flake normal. Aspecular lines are not suitable for this goal, since they simultaneously vary both the angle of

incidence with respect to the flake normal and the orientation angle of flakes sampled by the measurement. Only for metallic samples, it makes sense to investigate both interference and aspecular lines, since metallic pigments have a reflectance factor that is constant for different angles of incidence with respect to the flake normal.

We found several examples in which flake-based parameters made it possible to understand which measurement geometries can be expected to yield very similar reflection data. Thus it was explained why the off-plane 45as25az90 geometry in the MA98 instrument gives reflection measurements very similar to those from the Zeiss-06 geometry, although these geometries differ substantially in the values of illumination angle and aspecular angle.

FUTURE WORK

Based on the positive results in this study on the concepts of flake-based parameters, we are planning to investigate to what extent these concepts can help to identify effect pigments and conventional absorption pigments in an effect coating.

By selecting a series of measurement geometries, in which the value of the θ_{flake} parameter is fixed while the value of the θ_{inc} parameter is varied, it is possible to specifically sample the interference character of the effect pigments. We expect that such a series of measurement geometries makes it possible to characterize effect pigments even better than with the interference lines defined in previous work and tested here.

Another interesting series of measurement geometries is found by systematically varying the value of the θ_{flake} parameter while keeping the value of the θ_{inc} parameter fixed. In that case, the flake reflection coefficients are kept constant, since light is incident on the flakes from a constant angle θ_{inc} with respect to the flake normal. Therefore any changes in reflection for geometries in this series can only originate in the medium surrounding the flakes. Such a series of measurement geometries should make a better characterization of noneffect pigments possible than with the aspecular lines proposed before. As shown in this article, the aspecular lines are not suitable for this.

ACKNOWLEDGMENTS

The authors acknowledge X-Rite for making the MA98 instrument available for tests.

1. Saris HJA, Gottenbos RJB, van Houwelingen H. Correlation between visual and instrumental colour differences of metallic paint films. *Color Res Appl* 1990;15:200–205.
2. Alman DH. Symposium on color and appearance instrumentation. *Color Res Appl* 1990;15:365–366.
3. Alman DH. Directional color measurement of metallic flake finishes. Proceedings of the Inter-Society Color Council Conference on Appearance, ISCC, Williamsburg, 1987. p 53–56.
4. ASTM E2194–03. Standard Practice for Multi-Angle Color measurement of Metal Flake Pigmented Materials. American Society for the Testing of Materials, West Conshohocken, PA; 2009.

5. ASTM E 2539–08, Standard Practice for Multiangle Color Measurement of Interference Pigments. American Society for the Testing of Materials, West Conshohocken, PA; 2009.
6. Cramer WR. Examples of interference and the color pigment mixtures green with red and red with green. *Color Res Appl* 2002;27:276–281.
7. Cramer WR. Der richtige Blickwinkel. *Farbe + Lack* 2006;112:26–30.
8. Cramer WR, Gabel PW. Das gewisse Etwas, Dreieckbeziehungen aus Bunt-, Aluminium- und Mica-Lackierungen. *Farbe + Lack* 2003;109:78–84.
9. Cramer WR. Effekte sichten und beziffern. *Farbe + Lack* 2002; 108:48–55.
10. Cramer WR, Gabel PW. Effektiv messen. *Farbe + Lack* 2001; 107:42–48.
11. Cramer WR, Gabel PW. Measuring special effects. *Paint Coat Ind* 2001;9:36–46.
12. Cramer WR. Magical Mixtures. *Paint Coat Ind* 1999;9:72–75.
13. Klein GA. *Industrial Color Physics*. New York: Springer; 2010.
14. Pfaff G. *Special effect pigments*. Hannover: Vincentz; 2008.
15. Gabel PW. Goniochromatic color measurement systems—The past 20 years. In: Chung R, Rodrigues A, editors. *The Ninth Congress of the International Colour Associations*. (Bellagham, WA) SPIE 2002; 4421:798–802.
16. Hupp H. *Qualitäts- und Prozesskontrolle gedruckter Interferenzefektfarben erster Generation*. PhD Thesis, Technischen Universität Darmstadt; 2008.
17. LeLoup F, Hanselaer P, Pointer M, Versluys J. Characterization of gonio-apparent colours. *Proceedings of the AIC Color Conference, AIC, Granada, 2005*. p 515–519.
18. Takagi A, Sato S, Baba G. Prediction of spectral reflectance factor distribution of color-shift paint finishes. *Color Res Appl* 2007; 32:378–387.
19. Kirchner E, van den Kieboom GJ, Njo L, Supèr R, Gottenbos R. Observation of visual texture of metallic and pearlescent materials. *Color Res Appl* 2007;32:256–266.
20. Dekker N, Kirchner EJJ, Supèr R, van den Kieboom GJ, Gottenbos R. Total appearance differences for metallic and pearlescent materials: Contributions from color and texture. *Color Res Appl* 2011;36:4–14.
21. Nisper J, Richardson T, Teunis B. Major advances in the reliable measurement of the color and appearance of special effect paints and coatings. *Contribution to the American Coatings Conference, 2008, Charlotte, USA*.
22. Kirchner E, van den Kieboom GJ, Supèr R. Accurate measurement of sparkle for effect coatings. *Proceedings of the AIC Interim Meeting, AIC, Stockholm, 2008*. Paper no 012.
23. Kirchner EJJ, Houweling J. Measuring flake orientation for metallic coatings. *Prog Org Coat* 2009;64:287–293.
24. ASTM Task force E12.12.06 - WK 1164, *Standard Practice for Multi-angle Color Measurement, Identification, and Characterization of Interference Pigments*, West Conshohocken, PA: ASTM International; 2006, draft.